Cytomegalovirus pUL50 is the multi-interacting determinant of the core nuclear egress complex (NEC) that recruits cellular accessory NEC components

Sonntag, Eric; Hamilton, Stuart T.; Bahsi, Hanife; Wagner, Sabrina; Jonjić, Stipan; Rawlinson, William D.; Marschall, Manfred; Milbradt, Jens

Download date / Datum preuzimanja: **2025-03-28**

Cytomegalovirus pUL50 is the multi-interacting determinant of the core nuclear egress complex (NEC) that recruits cellular accessory NEC components

Eric Sonntag,[1] Stuart T. Hamilton,[2] Hanife Bahsi,[1] Sabrina Wagner,[1] Stipan Jonjic,[3] William D. Rawlinson,[2] Manfred Marschall[1] and Jens Milbradt[1]

Correspondence
Jens Milbradt
jens.milbradt@viro.med.uni-erlangen.de

[1]Institute for Clinical and Molecular Virology, Friedrich-Alexander University of Erlangen-Nürnberg (FAU), Erlangen, Germany

[2]Virology Division, SEALS Microbiology, Prince of Wales Hospital, Sydney, Australia

[3]Department of Histology and Embryology, Faculty of Medicine, University of Rijeka, Rijeka, Croatia

Nuclear egress of herpesvirus capsids through the nuclear envelope is mediated by the multimeric nuclear egress complex (NEC). The human cytomegalovirus (HCMV) core NEC is defined by an interaction between the membrane-anchored pUL50 and its nuclear co-factor pUL53, tightly associated through heterodimeric corecruitment to the nuclear envelope. Cellular proteins, such as p32/gC1qR, emerin and protein kinase C (PKC), are recruited by direct interaction with pUL50 for the multimeric extension of the NEC. As a functionally important event, the recruitment of both viral and cellular protein kinases leads to site-specific lamin phosphorylation and nuclear lamina disassembly. In this study, interaction domains within pUL50 for its binding partners were defined by co-immunoprecipitation. The interaction domain for pUL53 is located within the pUL50 N-terminus (residues 10–169), interaction domains for p32/gC1qR (100–358) and PKC (100–280) overlap in the central part of pUL50, and the interaction domain for emerin is located in the C-terminus (265–397). Moreover, expression and formation of core NEC proteins at the nuclear rim were consistently detected in cells permissive for productive HCMV replication, including two trophoblast-cell lines. Importantly, regular nuclear-rim formation of the core NEC was blocked by inhibition of cyclin-dependent kinase (CDK) activity. In relation to the recently published crystal structure of the HCMV core NEC, our findings result in a refined view of NEC assembly. In particular, we suggest that CDKs may play an important regulatory role in NEC formation during HCMV replication.

INTRODUCTION

Human cytomegalovirus (HCMV) is a globally human pathogen that infects immunocompetent individuals mostly without producing overt symptoms, whereas it is a major cause of morbidity and fatal disease in immunocompromised patients. Moreover, HCMV is the leading non-genetic cause of congenital malformation in developed countries. HCMV infection causes serious sequelae in immunocompromised patients and the developing foetus during pregnancy (Hamilton *et al.*,

2014). HCMV seroprevalence ranges from 40 % in highly industrialized areas to 90 % in developing countries (Adler *et al.*, 2007; Mocarski *et al.*, 2013). In general, HCMV and other herpesviruses undergo a cascade-like regulated replication, which is initiated in the host cell nucleus (Ogawa-Goto *et al.*, 2003). Thereafter, preformed viral capsids, packaged with genomic DNA, have to be translocated into the cytoplasm. Due to their large size (~130 nm), HCMV capsids are not able to pass the nuclear pore complex and a widely accepted mechanism for nuclear egress is considered by which viral capsids bud through nuclear membranes (Johnson & Baines, 2011; Mettenleiter *et al.*, 2013). To gain access to the inner nuclear membrane (INM), capsids need to traverse the

nuclear lamina, which underlies the INM. The nuclear lamina comprises a dense meshwork of nuclear lamins and lamina-associated proteins, and represents a natural barrier for viral nuclear egress. Thus, the nuclear lamina needs to be disassembled during herpesviral replication by the action of a viral–cellular multimeric-protein complex, termed nuclear egress complex (NEC) (Milbradt *et al.*, 2009). The recruitment of protein kinases to the NEC leads to the phosphorylation of lamins and thereby to a partial disassembly of the nuclear lamina. Notably, the core of the HCMV-specific NEC is formed by two conserved viral proteins, pUL50 and pUL53. The integral membrane protein pUL50 is associated with the INM by its transmembrane domain, whereas the nuclear phosphoprotein pUL53 carries a classical nuclear localization signal (NLS, aa 18–27) (Schmeiser *et al.*, 2013) and accumulates in a nuclear rim localization upon interaction with the INM-associated pUL50. A currently accepted concept is that pUL50 and pUL53, as well as their α-, β- and γ-herpesviral homologues, are functionally essential for nuclear capsid egress, with the exception of distinct alphaherpesviral mutants reinforcing an

alternative egress pathway based on nuclear envelope breakdown (Klupp *et al.*, 2011; Grimm *et al.*, 2012). Once the core NEC is formed, further NEC proteins like p32/gC1qR, emerin and additional candidates are recruited (Milbradt *et al.*, 2014). Among these, viral protein kinase pUL97, cellular protein kinase C isoform α (PKCα) and possibly others are recruited (Milbradt *et al.*, 2007, 2009) in order to phosphorylate nuclear lamins resulting in lamina disassembly (Hamirally *et al.*, 2009; Milbradt *et al.*, 2010). The recently solved crystal structure of the pUL50-pUL53 complex suggests that pUL50-pUL53 heterodimers assemble to hexameric ring-like structures, acting as a scaffold for binding of further NEC proteins (Walzer *et al.*, 2015). Hence, the NEC represents an attractive and promising target for antiviral drug development. It has been shown previously that inhibition of pUL97 activity, in particular pUL97-mediated core NEC phosphorylation, led to a significant reduction of viral titres, underlining the importance of proper NEC formation (Prichard *et al.*, 1999; Wolf *et al.*, 2001; Krosky *et al.*, 2003; Marschall *et al.*, 2005; Sharma *et al.*, 2015).

In this study, we provide a closer insight into the HCMV-specific NEC formation. By performing co-immunoprecipitation (CoIP) experiments, we identified four partly distinct, partly overlapping pUL50-interaction domains being necessary and sufficient for interaction with the NEC components pUL53, p32/gC1qR, emerin and PKCα. Expression of pUL50-pUL53 and core NEC formation was demonstrated in human cell types comprising variable levels of HCMV permissiveness, also including trophoblast cell lines. In addition, nucleoplasmic relocalization of pUL53 from the nuclear rim was demonstrated upon inhibition of cellular cyclin-dependent kinase (CDK) activity in HCMV-infected and plasmid-transfected cells. Combined, our data support an extended model of NEC formation, primarily based on four interaction domains in pUL50, also including the relevance of cell type, cellular pUL50-associated NEC proteins and cellular kinase activity.
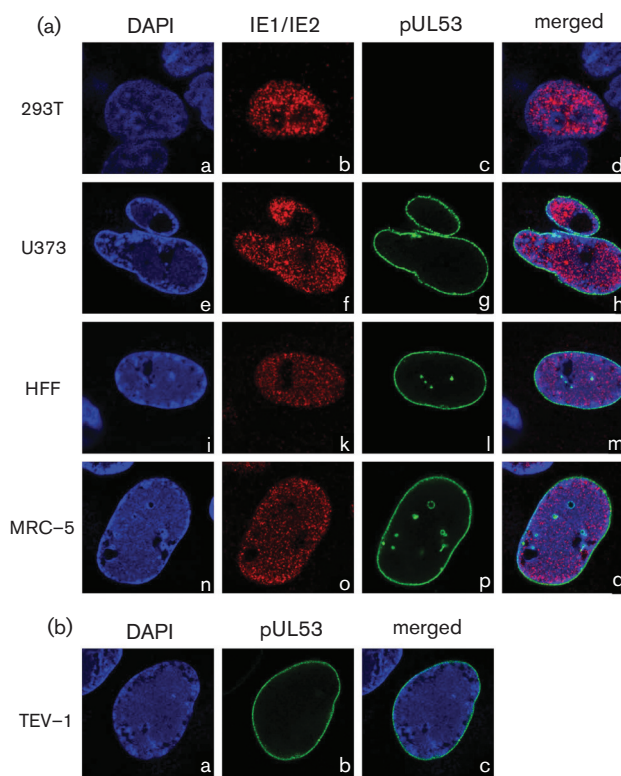

Fig. 1. Nuclear rim localization of the core NEC in HCMV-permissive and -non-permissive cell types. Infection of (a) 293T, U373, HFF, MRC-5 and (b) TEV-1 cells with HCMV strain AD169 at a MOI of 1. At 3 dpi, cells were fixed and co-immunostained with antibodies directed against HCMV immediate-early proteins 1 and 2 (IE1/IE2) or pUL53 as indicated. Nuclei were counterstained by DAPI (4,6-diamidino-2-phenylindole). Samples were analysed by confocal microscopy.

RESULTS

Expression pattern of core NEC proteins and nuclear rim formation is a common feature among HCMV-permissive cells, but shows variation in poorly permissve cell types

Coordinated NEC formation is a crucial step in HCMV replication. Initially, pUL50 is produced with early-phase kinetics, translocated into the nucleus, and accumulates at the INM to recruit other cellular and viral components involved in nuclear lamina reorganization (Hamirally *et al.*, 2009; Milbradt *et al.*, 2010; Schmeiser *et al.*, 2013). We addressed the question of whether NEC formation may vary between different host cell types being HCMV-permissive (HFF, MRC-5), semi-permissive (U373, TEV-1) or non-permissive for productive replication in cell culture (293T). Experiments were performed using HCMV strain AD169 at a multiplicity of infection (MOI) of 1. Three days

post-infection (dpi), intracellular pUL53 localization was compared to that of viral immediate-early proteins (IE1 and IE2) by confocal microscopy (Fig. 1). All cell types used showed IE1/IE2 expression, indicating consistently successful viral entry and onset of viral gene expression (Fig. 1a) (notably, regular IE1/IE2 expression in HCMV-infected TEV-1 cells was detected in a control experiment, *data not shown*). Moreover, pUL53 was detected in U373, HFF, MRC-5 (Fig. 1a) and TEV-1 cells (Fig. 1b). On the contrary, 293T cells were negative for pUL53, indicating that viral replication is impeded in this cell type (confirming earlier data by Ellsmore *et al.*, 2003).

In a following step, we performed Western blot kinetic experiments to monitor the presence of pUL50 and pUL53 along the course of infection (Fig. 2). At consecutive time points, IE1 production was detectable starting from 1 dpi in all cell types analysed (Fig. 2a). This also included 293T cells in which, however, later viral proteins were missing. Notably, the semi-permissive U373 cells expressed only marginal levels of pUL50 and pUL53 at a delayed kinetic (Fig. 2a, lanes 9−10). In comparison, the placental cell line TEV-1 showed a stronger level of core NEC expression at late time points of infection (lanes 14−15). Interestingly, the infection rate of TEV-1 cells also varied between different HCMV strains, indicated by variable expression patterns of viral IE, early (E) and late (L) proteins (Fig. 2a). Another placental cell line, JEG3, showed a variable expression of E proteins (i.e. reduced levels of pUL44; pUL50 and pUL53 expression was under the detection limit) upon infection with HCMV strain AD169 (propagated in HFFs). Moreover, JEG3 cells completely lacked expression of the L major capsid protein (MCP) (Fig. 2c). In contrast, HCMV proteins were consistently and strongly expressed in HFF and MRC-5 fibroblasts at 3 dpi (Fig. 2a, lanes 16−25). Thus, our findings indicate that the expression of core NEC proteins and nuclear rim formation is conserved in cells permissive for productive HCMV replication.

Core NEC formation is sensitive to inhibitors of CDK activity

As demonstrated in detail by previous confocal imaging analyses (Milbradt *et al.*, 2012; Schmeiser *et al.*, 2013; Sharma *et al.*, 2015), pUL50 and pUL53 recruit each other into a nuclear rim-associated NEC structure. Notably, this rim colocalization is blocked by treatment with the pUL97-specific inhibitor maribavir (MBV) (Sharma *et al.*, 2015). In this study, we looked at whether or not inhibitors of cellular kinases similarly block core NEC formation at the nuclear rim. CDK inhibitors were suspected as candidates, since CDKs and pUL97 are considered as orthologues, sharing properties of cyclin binding, substrate phosphorylation and regulatory functions in HCMV replication (Hume *et al.*, 2008; Graf *et al.*, 2013; Steingruber *et al.*, 2015). For this purpose, we infected HFFs with the recombinant HCMV AD169-GFP UL50-HA expressing the green fluorescent protein (GFP) as a marker of infected cells and pUL50 fused

to an HA-tag. Infected cells were cultivated in the presence or absence of the CDK inhibitors R25 (also known as Alsterpaullone), R22 or LDC4297 (Fig. 3a). Control cells (DMSO, dimethyl sulfoxide) and cells treated with the CDK9-specific inhibitor R22 or CDK7-specific inhibitor LDC4297 displayed regular rim co-localization of pUL50 with pUL53 (Fig. 3a, panels a–d and i–q). Notably, z-series of corresponding areas revealed that some cells showed co-localization of pUL50 and pUL53 in tubular structures spanning the nucleus from the bottom to the top (e.g. *open arrows* in xz and yz sections of Fig. 3a, panels d, m and q). These tubular structures are common in human fibroblasts and represent transnuclear channels of nuclear membrane invaginations which allow transport between different cytoplasmic regions (Broers *et al.*, 2006). Intriguingly, we additionally observed intranuclear aggregates of pUL50-pUL53 co-localization under R25 treatment (Fig. 3a, panels e–h), but not under treatment with R22 or LDC4297 (panels i–q). In contrast to the nucleus-spanning tubules, these are distinct aggregates adjacent to the nuclear rim but not continuous with the nuclear membrane (see *yellow-filled arrows* in xz and yz sections of Fig. 3a, panel h). This R25-mediated phenotype was specifically pronounced for pUL53. Interestingly, treatment with the pUL97 inhibitor MBV resulted in similar intranuclear aggregates of pUL50 and pUL53 (Fig. 3a, panels r–u). Notably, R25 has activity against CDKs including CDK1, CDK2 and CDK5 (Sandal *et al.*, 2002; Soni & Jacobberger, 2004), but it does not block pUL97-mediated substrate phosphorylation (Sonntag, E., Marschall, M. & Milbradt, J., *unpublished data*).

To verify that the observed effect in R25-treated cells is independent of the viral protein kinase pUL97, we studied pUL50 and pUL53 localization in transfected HeLa cells (Fig. 3b). As expected, MBV treatment had no effect on the nuclear rim co-localization of pUL50 and pUL53 compared with DMSO-treated control cells in the absence of pUL97 or other viral proteins (Fig. 3b, panels a–d and r–u). However, the addition of R25 changed the nuclear rim localization of pUL50 and pUL53 also in transfected cells. In particular, R25 treatment induced intranuclear aggregates of pUL53 and pUL50 adjacent to the nuclear rim in 61.9 % of investigated cells (Fig. 3b, panels e–h). Similar to HCMV infection, the effect of R25 in transfected cells was more pronounced for pUL53. Moreover, LDC4297 treatment also induced re-localization of pUL50 and pUL53 in transfected cells, albeit at lower efficacy (Fig. 3b, panels i–m). In contrast, treatment with R22 did not induce similar changes so that core NEC proteins remained in their original nuclear rim co-localization (Fig. 3b, panels n–q).

In a next step, we performed co-immunoprecipitation (CoIP) analysis to establish whether or not specific CDKs are directly associated with the viral core NEC. Importantly, pUL50 was able to co-immunoprecipitate CDK1 from lysates of transiently transfected 293T cells (Fig. S1, available with the online supplementary material). The detectability of CDK1-pUL50 interaction, however, varied between individual experiments and the functional importance of this interaction remains to be clarified. As seen
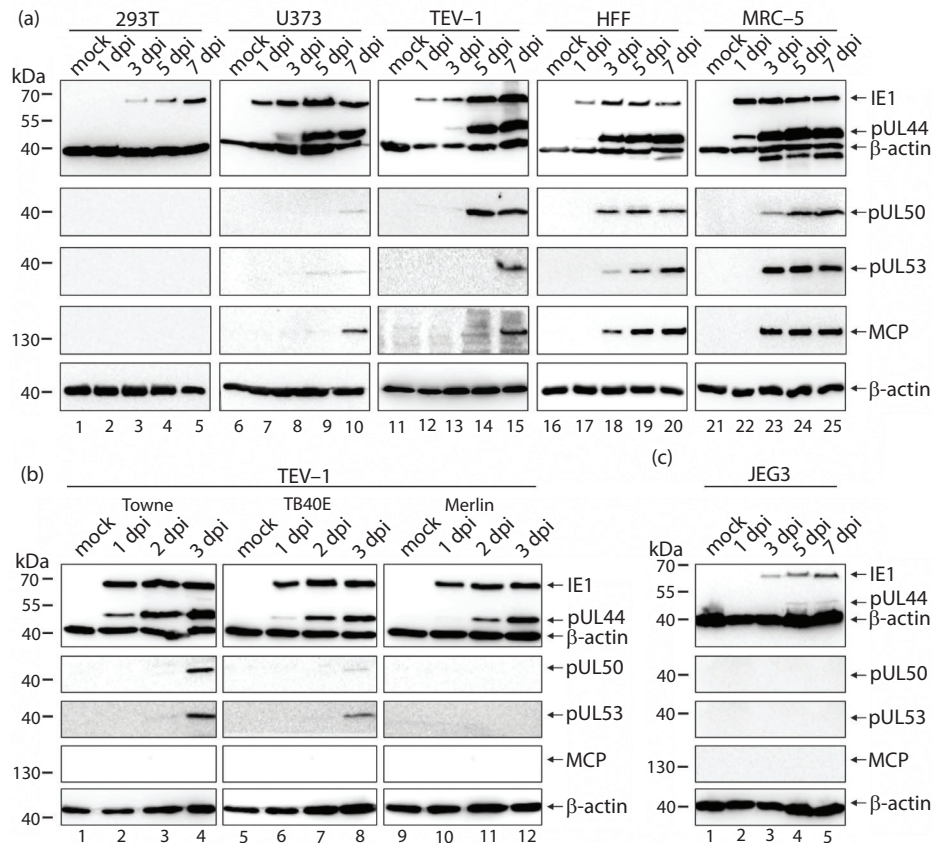
Fig. 2. Viral protein expression in cell types differentially permissive for HCMV. Various cell types were infected with HCMV strain AD169 at a MOI of 1 (a), at a MOI of 10 (c), or were infected with HCMV strains Towne, TB40E and Merlin at a MOI of 1 (b) as indicated. Cells were harvested and lysed at consecutive time points post-infection, shown above blots. Expression levels of IE1 (splice variant IE1p72), early (pUL44, pUL50, pUL53) and late proteins (MCP) were analysed by Western blot analyses using protein-specific antibodies.

from the current state of analysis, both results derived from the CoIP and the confocal kinase inhibitor studies suggest the involvement of CDKs in core NEC formation. Taken together, our findings provide the first evidence that core NEC formation is sensitive to CDK inhibitors and may thus be directly dependent on CDK activity.

Localization of individual constituents of the multimeric NEC is differentially sensitive to the CDK inhibitor R25

The core NEC recruits further proteins to form a multimeric NEC at the late stages of HCMV replication (Milbradt et al., 2014). Thus, we investigated the effect of R25 on the subcellular localization of further components of the multimeric NEC, namely p32/gC1qR (Fig. 3c) and emerin (Fig. 3d). p32/gC1qR is a predominant mitochondrial protein that can accumulate in the nucleus under specific stimuli (Brokstad et al., 2001). Notably, p32/gC1qR localization changed from a tubular cytoplasmic localization

in uninfected cells (mock) to a partial translocation into the nucleus during HCMV replication (Fig. 3c, compare panels i–m to panels a–d), confirming previous results (Milbradt et al., 2014). Intriguingly, inhibition of CDK activity by R25 treatment decreased the nuclear abundance of p32/gC1qR but led to a partial co-localization with pUL53 in the inhibitor-induced intranuclear aggregates (Fig. 3c, panels e–h). However, R25 treatment showed the reciprocal phenotype of an increased nuclear translocation in uninfected cells compared to DMSO treatment (Fig. 3c; compare panels n–q to panels i–m). This finding was unexpected and pointed to a complex regulation of NEC constituents by cellular and viral protein kinases. In contrast to p32/gC1qR, emerin did not show similarly altered localization following R25 treatment (Fig. 3d). In conclusion, localization of specific NEC constituents is either directly or indirectly regulated by CDK activity during HCMV replication. Moreover, it appears highly likely that multiple events of phosphorylation are required for proper formation of the multimeric NEC.
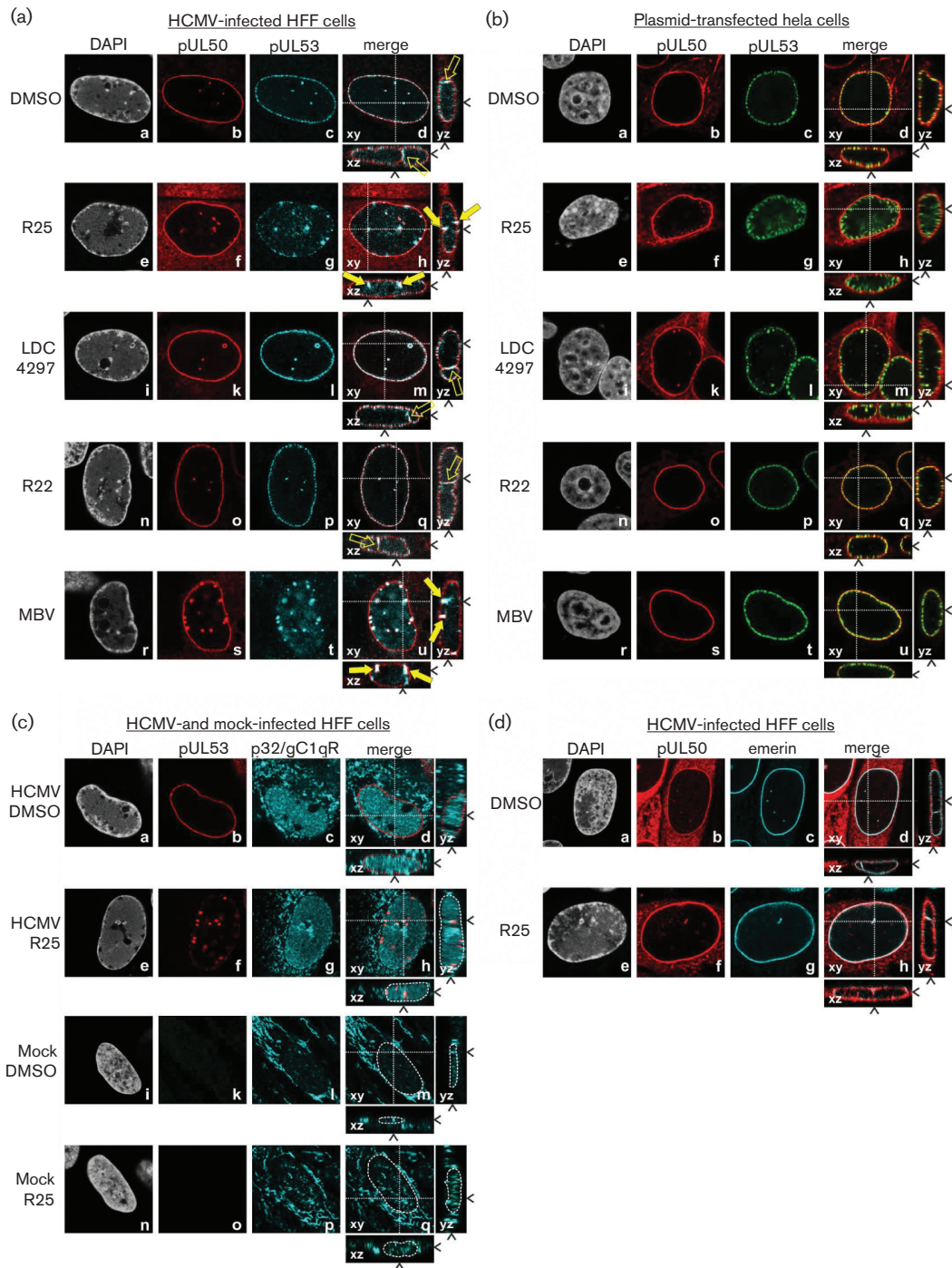
Fig. 3. Effect of CDK inhibitors on NEC formation. (a,c,d) HFFs were infected with recombinant HCMV AD169-GFP UL50-HA at a MOI of 1 or remained uninfected (mock). (b) HeLa cells were transiently co-transfected with plasmids coding for HA-tagged pUL50 or FLAG-tagged pUL53. (a-d) The protein kinase inhibitors R25 (3 μm), R22 (3 μm), LDC4297 (0.5 μm), maribavir (MBV, 5 μm) or DMSO were added to infected cells at 74 and 94 h post-infection (hpi) (a,c,d) and to transfected cells directly after plasmid transfection (b). Infected and transfected cells were fixed at 96 hpi (a,c,d) and 48 h post-transfection (b), respectively, and subjected to indirect immunofluorescence analysis using protein- or tag-specific antibodies. The subcellular localization of viral pUL50 and pUL53, as well as cellular p32/gC1qR and emerin, was detected by recording confocal z-series. Representative images of a single focal plane (xy) are depicted for individual stainings. In addition, xz and yz axes are depicted for merged images. *White dotted lines and black arrowheads*, optical section through the z stack (xy) or the focal plane (xz and yz); *yellow-filled arrows*, intranuclear aggregates of pUL50/pUL53 co-localization; *yellow open arrows*, transnuclear transport channels common in fibroblasts.

Functional map of pUL50 regions determining its binding to pUL53, PKCα, p32/gC1qR and emerin

Various lines of experimental evidence suggested that the cytomegaloviral core NEC acts as a scaffold to assemble accessory NEC components (Muranyi *et al.*, 2002; Milbradt *et al.*, 2007, 2009, 2014; Buchkovich *et al.*, 2010; Lemnitzer *et al.*, 2013). In particular, pUL50 defines the formation of the multimeric NEC by interacting with pUL53, PKCα, p32/gC1qR and emerin. Previously, we used either N- or C-terminally truncated versions of pUL50 to determine the interaction domains facilitating its multiple interactions (Milbradt *et al.*, 2009, 2014). In this study, we generated expression constructs coding for specific regions of pUL50 and analysed these in respect of their binding characteristics by CoIP assay (Fig. 4a–d). Specifically, residues 10–169 of pUL50 were sufficient for pUL53 CoIP (Fig. 4a, lane 4), whereby the quantity of interaction signals was reduced in comparison to the full-length protein (Fig. 4a, compare lane 3 with lane 4). The specificity of CoIP reactions was assured by the use of an Fc fragment as control (Fig. 4a, lane 1). For interaction with PKCα and p32/gC1qR, responsible regions of pUL50 were mapped to partly overlapping interaction domains comprising residues 100–280 (Fig. 4b, lanes 2 and 3) and residues 100–358 (Fig. 4c, lanes 2 and 3), respectively. Distinct from these interaction domains, the region responsible for emerin interaction was mapped to the C-terminus of pUL50 (Fig. S2). In particular, residues 265–397 of pUL50 were sufficient to confer emerin interaction (Fig. 4d, lanes 3 and 4), whereby C-terminal truncation abolished interaction (Fig. S2, lanes 9–11). The resulting interaction domains were evaluated as specific, since we did not observe cross-interaction with emerin (Fig. 4a–c, lane 3 or 4) or PKCα (Fig. 4d, lane 4). Staining of lysate controls demonstrated comparable levels of transiently expressed proteins (Fig. 4a–d, lower panels). A summary of CoIP data is presented schematically (Fig. 5a), illustrating the partly overlapping pUL50 interaction domains for pUL53, PKCα, p32/gC1qR and emerin. It should be stressed that Fig. 5b shows a partial inset of the recently resolved crystal structure of the pUL50-pUL53 heterodimeric complex (Walzer *et al.*, 2015). Residues 10–169 of pUL50, representing the minimal interaction domain for pUL53, are displayed in green; residues 50–84 of pUL53 forming an N-terminal hook-like extension determining interaction in red. Primary and secondary structural features of pUL50 are depicted in Fig. 5c. Intriguingly, for the C-terminal part of pUL50 stretching outside the globular domain (comprising residues 1–209) (Milbradt *et al.*, 2012), only a few secondary structural elements were predicted, so that this disordered region appears to be mostly unstructured. This is even more remarkable considering the finding that the main part of the three overlapping interaction domains for PKCα, p32/gC1qR and emerin is almost entirely contained within the C-terminal half of the protein (Fig. 5c). Combined, this structural and functional arrangement of four interaction domains spanning pUL50 is a highly interesting feature that has not been recognized to date. Thus, the unique assembly properties of pUL50 may define its central role in scaffolding multimeric interactions of viral and cellular proteins within the cytomegalovirus-specific NEC.

DISCUSSION

In this study, we provide novel insights into the assembly of the HCMV-specific multimeric NEC and the defining role of the core NEC constituent pUL50. We used biochemical methods including CoIP analyses and confocal microscopy to explore the recruitment and interaction of NEC components in various host cell types and a potential role of cellular CDKs for efficient NEC formation. The main findings are: (i) the core NEC is formed in HCMV-permissive host cells; (ii) treatment with CDK inhibitors impairs efficient core NEC formation in HCMV-infected cells; and (iii) pUL50 defines the assembly of the multimeric NEC by partly distinct and partly overlapping interaction domains for accessory NEC components.

Assembly of the core NEC is characterized by an interaction-driven recruitment of pUL50 and pUL53, resulting in their perfect co-localization at the nuclear envelope of HCMV-infected cells (Schmeiser *et al.*, 2013, 2015). Here, we investigated nuclear rim formation of pUL53 in various cell types which are differentially permissive for HCMV infection. In semi-permissive (U373, TEV-1) and fully permissive cells (HFF, MRC-5), pUL53 is perfectly localized at the nuclear rim. In line with our Western blot results, reliable levels of expression of the two core NEC proteins were detected in these cells by confocal microscopy. Interestingly, expression of pUL50 and pUL53 was also detected in trophoblast cells, but TEV-1 and JEG3 cells showed slight differences in expression patterns of both proteins during infection. A possible reason for this is that TEV-1 and JEG3 cells differ in their developmental stages (i.e. transformed extra-villious first-trimester cells or choriocarcinoma cells, respectively). Moreover, confocal microscopy demonstrates rim staining of pUL53 in HCMV-infected cells, indicating core NEC formation also in trophoblast cells. On the contrary, 293T cells are known to be non-permissive for the production of infectious HCMV. Nevertheless, we detected viral IE protein expression following HCMV infection, while expression of E proteins, including pUL50 and pUL53, and L proteins was missing. This confirms earlier findings, illustrating that the viral replication cycle is impeded in 293T cells and the course of infection is abortive (Ellsmore *et al.*, 2003). In addition to the cell type-specific differences in core NEC expression, we also demonstrated that the time course of NEC formation is dependent on HCMV strains (Dolan *et al.*, 2004). Notably, our data exemplify that the onset of expression of core NEC proteins in TEV-1 cells slightly differed between the HCMV strains analysed. Thus, our findings indicate that nuclear rim formation and expression of core NEC proteins show some degree of cell type- and viral strain-specific variation, but are conserved for cells permissive for productive HCMV infection.
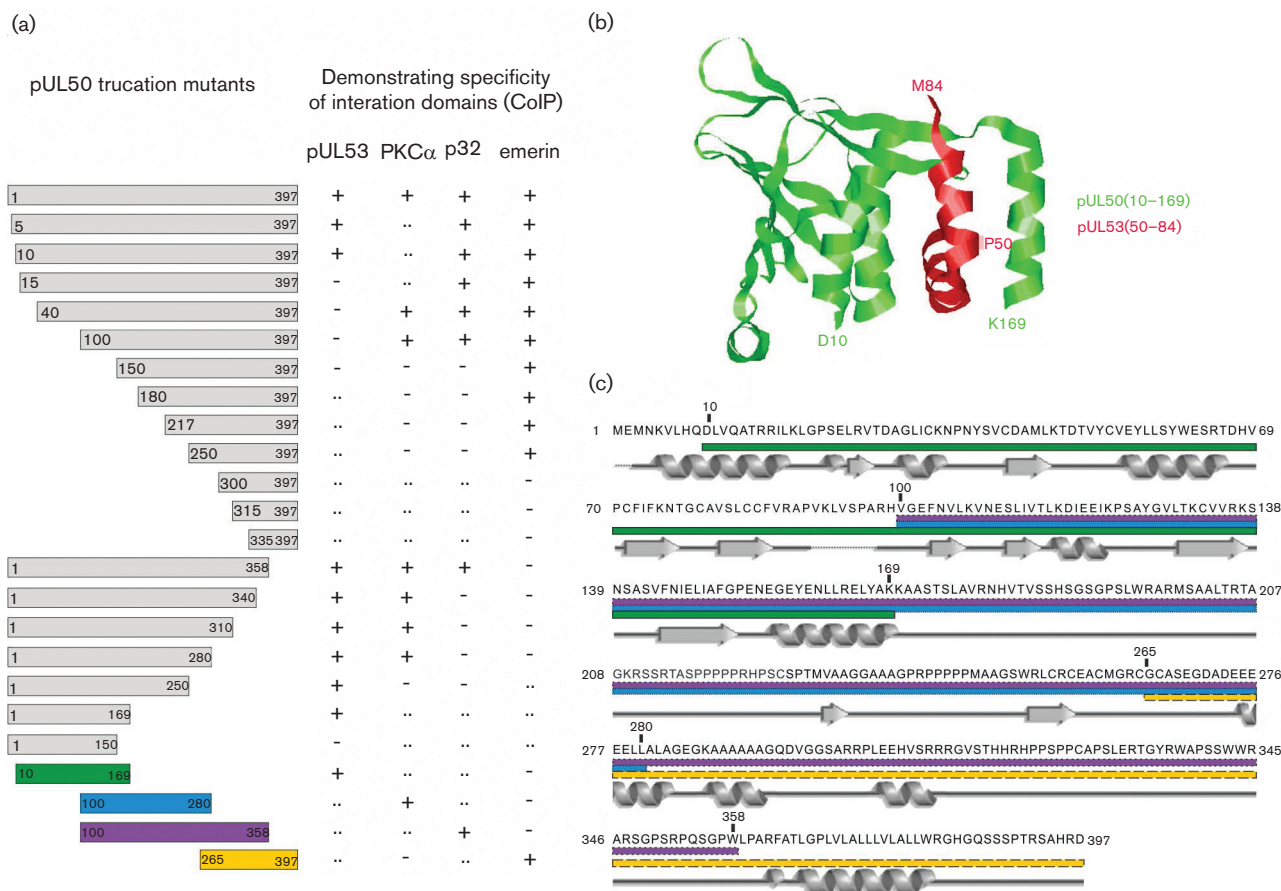
Fig. 5. Regions and secondary structural elements determining binding properties of pUL50. (a) Schematic presentation of CoIP data obtained with N- and C-terminal truncation mutants of pUL50 (this study and Milbradt *et al.*, 2009, 2012, 2014). Note, specific regions of pUL50 responsible for interaction with pUL53 (green), PKCα (blue), p32 (purple) and emerin (yellow). +, CoIP positive; −, CoIP negative; ••, not determined. (b) Ribbon presentation of the reciprocal interaction domains comprised in the recently solved crystal structure of the pUL50-pUL53 core NEC (PDB code 5D5N; Walzer *et al.*, 2015): pUL53 interaction domain within pUL50 (amino acids 10−169) depicted in green, pUL50 interaction domain within pUL53 (amino acids 50−84) (Sam *et al.*, 2009) depicted in red. (c) Schematic presentation of the pUL50 secondary structure. Secondary structure prediction of amino acids 172–397 was performed with the JPred 4 (http://www.compbio.dundee.ac.uk/jpred/) prediction tool. Secondary structural elements contained within amino acids 1–171 are derived from the crystal structure (b). Identified interaction domains within pUL50 are highlighted by shaded boxes (green, pUL53; blue, PKCα; purple, p32; yellow, emerin).

Regular NEC formation is dependent on pUL50-pUL53 heterodimerization (Milbradt *et al.*, 2012; Sam *et al.*, 2009; Walzer *et al.*, 2015) and post-translational protein modification (Sharma *et al.,* 2015). Phosphorylation of pUL50 and pUL53 by the HCMV-encoded protein kinase pUL97 is essential for proper nuclear rim localization. In particular, Sharma and colleagues demonstrated that an inhibitor-mediated block of pUL97 results in a significant reduction in viral titres and, moreover, leads to a punctate distribution of both pUL50 and pUL53 (Sharma *et al.,* 2015). Recent reports from our group suggested functionally relevant cyclin interaction of the viral kinase pUL97 (Graf *et al.*,

2013; Steingruber *et al.*, 2015), further substantiating the role of pUL97 as a viral CDK ortholog (Hume *et al.*, 2008).

Besides HCMV pUL97, regulation of NEC formation and function by cellular kinases has been discussed in various aspects (Marschall *et al.*, 2011). On the one hand, a functional role of cellular PKCα in the virus-mediated nuclear lamina disassembly during infection with HCMV and other herpesviruses has been suggested (Muranyi *et al.*, 2002, 2009, 2010; Leach & Roller, 2010). Moreover, PKCα phosphorylates pUL50 *in vitro* (Milbradt *et al.*, 2007). On the other hand, it is tempting to speculate that cellular CDKs additionally regulate the NEC. Previous studies

demonstrated the general importance of CDK activity for efficient HCMV replication (Schang et al., 2005; Sanchez & Spector, 2006; Hertel et al., 2007). To address whether or not CDKs regulate core NEC formation, we blocked CDK activity by treatment of HCMV-infected cells with known CDK inhibitors. Importantly, pUL53 and pUL50 were partially re-localized from their nuclear rim localization into the nucleoplasm of HCMV-infected cells following treatment with 3 μm of the CDK inhibitor R25 (i.e. R25 blocks activity of CDK1, CDK2 and CDK5) (Sandal et al., 2002; Soni & Jacobberger, 2004). Consistent with our data, R25 treatment has been shown to reduce viral titres by approximately 1.2 log units, even at a much lower dose of 150 nM (Bigley et al., 2015). The identification of the CDK1-pUL50 interaction by CoIP analysis in the present study further suggests that at least CDK1 is directly involved in core NEC formation. Hertel and colleagues previously showed that inactivation of CDK1 alone is not sufficient to reduce viral titres, but a broader set of CDK activities is important for efficient progression of HCMV replication (Hertel et al., 2007). Thus, our data suggest that the concerted action of cellular CDKs in addition to the viral kinase pUL97 is essential for regular NEC assembly. In addition to the inhibition of CDKs, R25 has activity against glycogen synthase kinase 3 (GSK3) isoforms. The potential functional relevance of GSK3 and Wnt signalling for NEC formation and nuclear egress remains to be elucidated in future studies.

In general, NEC formation is a tightly regulated multi-step process which consists of the recruitment of several cellular and viral proteins. Previously, we identified the most important players for the formation of the HCMV-specific multimeric NEC: viral core NEC proteins pUL50–pUL53, cellular targeting and adaptor proteins emerin and p32/gC1qR, as well as the lamin-phosphorylating protein kinases pUL97 and PKCα (Milbradt et al., 2009, 2014). In the present study, we elucidated pUL50 regions that are required for NEC formation. Importantly, the pUL50 N-terminus is essential for pUL53 binding, and thus sufficient for core NEC formation. In line with this finding, the recently resolved crystal structure of the pUL50-pUL53 core NEC demonstrated that this portion of pUL50 actually displays the central interaction surface for pUL53 (Lye et al., 2015; Walzer et al., 2015). For PKCα and p32/gC1qR, the interaction domains are partly located within the globular central part, but extend into the disordered C-terminus of pUL50. The interaction domain for emerin is completely located within the disordered C-terminus. Hence, the pUL50 C-terminus emerges as an essential scaffold for the formation of the multimeric NEC.

In summary, our results suggest that core NEC formation, on the basis of pUL50-pUL53 heterodimerization and strict nuclear rim recruitment, is a conserved process in HCMV-permissive cells. In this regard, the pUL50 N-terminus is sufficient for core NEC formation with pUL53, while central and C-terminal parts of pUL50 determine interaction with further constituents of the HCMV-specific multimeric NEC. Importantly, inhibitor experiments suggested that

NEC formation is regulated by cellular CDK activity. Taken together, these findings provide novel insights into NEC formation during HCMV infection and might be used to develop novel strategies for future therapeutic intervention.

METHODS

Plasmid constructs. Expression plasmids coding for haemagglutinin (HA)-tagged truncation mutants of HCMV pUL50 were generated by PCR amplification of the UL50 open reading frame. N-terminal (i.e. encoding amino acids 180–397, 217–397 or 265–397) as well as N- and C-terminal truncation mutants of pUL50 (encoding amino acids 10–169, 100–280, or 100–358) were generated by cloning of PCR products. Standard PCR amplification was performed using pcDNA-UL50-HA (Milbradt et al., 2007) as a template and oligonucleotide primers purchased from Biomers (Ulm, Germany); sequences of oligonucleotides are given in supplemental Table S1. After cleavage with EcoRI/XhoI, PCR products were inserted into the eukaryotic expression vector pcDNA3.1 (Life Technologies). Expression plasmids coding for the following HA- or FLAG- (Asp-Tyr-Lys-Asp-Asp-Asp-Asp-Lys)-tagged versions of HCMV and cellular proteins were described previously: HCMV proteins pUL53-FLAG, pUL50-HA, pUL50(5–397) and pUL50 (40–397); cellular PKCα-FLAG and p32(50–282) (Milbradt et al., 2007, 2009, 2012).

Cell culture, plasmid transfection and human cytomegalovirus infection. Human embryonic epithelial kidney (HEK) 293T cells and neuronal glioblastoma U373-MG cells were cultivated in Dulbecco's modified Eagle's medium (DMEM), containing 10 % foetal calf serum (FCS) and 100 mg ml^{-1} gentamicin. Primary human foreskin fibroblasts (HFF), embryonic lung fibroblasts MRC-5 and cervix carcinoma epithelial HeLa cells were cultivated in minimal essential medium (MEM) containing 7.5 % FCS and 100 mg ml^{-1} gentamicin. Human first-trimester extra-villous trophoblast TEV-1 cells and human placental choriocarcinoma JEG3 cells were cultured in DMEM/F-12+Gluta-aMAX, supplemented with 10 % FCS and 1X PSG (kindly provided by the laboratory of Prof. William D. Rawlinson, Virology Division, SEALS Microbiology, Prince of Wales Hospital, Sydney, Australia). Transient transfection in 293T cells was performed by the use of polyethylenimine–DNA complexes (Sigma-Aldrich) as described previously (Schregel et al., 2007). HeLa cells were transfected using Lipofectamine 2000 (Life technologies) according to the manufacturer's instructions. HCMV infection experiments were performed at a MOI of 1.0 (or higher as indicated for specific experiments) using HCMV strains AD169, AD169-GFP UL50-HA (Schmeiser et al., 2013), Towne, TB40E and Merlin. After incubation for 90–120 min at 37 °C, virus inoculi were removed and replaced with fresh growth medium.

Protein kinase inhibitors. The drugs used in the present study were obtained from various sources: the CDK inhibitors R25 (also known as Alsterpaullone) (Rechter et al., 2009) and R22 (Feichtinger et al., 2011) were provided by GPC Biotech AG (Martinsried, Germany), the CDK7-specific inhibitor LDC4297 (Hutterer et al., 2015) was provided by Lead Discovery Centre GmbH (Dortmund, Germany), and maribavir (MBV), a specific inhibitor of the HCMV protein kinase pUL97 (Trofe et al., 2008; Chou et al., 2012), was purchased from Shanghai PI Chemicals Ltd (China). The compounds were dissolved in dimethyl sulfoxide (DMSO) and stored at −20 °C according to the manufacturer's instructions.

Antibodies. Monoclonal (mAb) and polyclonal (pAb) antibodies, mouse pAb-HA (T501, Signalway Antibody LLC, College Park, MD, USA), mouse mAb-HA (clone HA-7, Sigma-Aldrich) and mouse mAb-FLAG (1804, Sigma-Aldrich) were used to detect transiently expressed HA- or FLAG-tagged proteins. Antibodies against HCMV proteins were

rabbit pAb-IE1/IE2 (Gebert *et al.*, 1997), mouse pAb-UL53 (kindly provided by Dr P. Dal Monte, Bologna, Italy), mouse mAb-UL50 (UL50.01; kindly provided by Prof. S. Jonjic and Dr T. Lenac, University of Rijeka, Croatia) and mouse mAb-UL44 (kindly provided by Prof. B. Plachter, University of Mainz, Germany). Additional antibodies against HCMV IE1p72 and MCP were kindly provided by William Britt (University of Alabama). Antibodies against cellular proteins were mouse mAb-emerin (H-12, Santa Cruz Biotech), rabbit pAb-p32 (kindly provided by Prof. W. C. Russel, St Andrews, UK), mouse mAb-cyclin B1 (D-11, Santa Cruz Biotech), rabbit pAb-cyclin B1 (H-433, Santa Cruz Biotech), rabbit pAb-CDK1 (cdc2 p34, C-19, Santa Cruz Biotech) and mouse mAb-β-actin (AC-15, Sigma-Aldrich). Secondary antibodies were Alexa Fluor 488-/555-conjugated secondary antibodies for indirect immunofluorescence (Molecular Probes) and horseradish peroxidase-conjugated anti-mouse/-rabbit secondary antibodies for Western blot analyses (Dianova, Hamburg, Germany).

Indirect immunofluorescence assay and confocal laser-scanning microscopy. HFFs or HeLa cells were seeded on coverslips for infection or transient transfection experiments. At indicated time points, cells were fixed and permeabilized following indirect immuno-fluorescence staining as described previously (Milbradt *et al.*, 2007, 2009). Images were acquired using a TCS SP5 confocal laser-scanning microscope (Leica Microsystems, Wetzlar, Germany). For three-dimensional images, z-series were recorded along 12 μm (*z*-axis) with a pinhole of 1 airy unit. Images and z-series were analysed using LAS AF software (Leica Microsystems, Wetzlar, Germany).

Co-immunoprecipitation (CoIP) assay. 293T cells were seeded into 10 cm dishes with a density of 5.0×10^6 cells. Two days post-transfection, cells were lysed in 500 μl CoIP buffer (50 mM Tris/HCl (pH 8.0), 150 mM NaCl, 5 mM EDTA, 0.5 % NP-40, 1 mM PMSF, 2 μg aprotinin ml^{-1}, 2 μg leupeptin ml^{-1} and 2 μg pepstatin ml^{-1}). Subsequently, total lysates were incubated with antibody-coated (2 μl of tag-specific or control antibodies) Dynabeads® Protein A (30 μl per sample; Life Technologies) for 2 h at 4 °C under rotation. The precipitates were washed five times with 1 ml CoIP buffer. CoIP samples and lysate controls taken prior to the addition of the CoIP antibody were subjected to standard Western blot analysis.

ACKNOWLEDGEMENTS

REFERENCES

Adler, S. P., Nigro, G. & Pereira, L. (2007). Recent advances in the prevention and treatment of congenital cytomegalovirus infections. *Semin Perinatol* **31**, 10–18.

Bigley, T. M., Reitsma, J. M. & Terhune, S. S. (2015). Antagonistic relationship between human cytomegalovirus pUL27 and pUL97 activities during infection. *J Virol* **89**, 10230–10246.

Broers, J. L., Ramaekers, F. C., Bonne, G., Yaou, R. B. & Hutchison, C. J. (2006). Nuclear lamins: laminopathies and their role in premature ageing. *Physiol Rev* **86**, 967–1008.

Brokstad, K. A., Kalland, K. H., Russell, W. C. & Matthews, D. A. (2001). Mitochondrial protein p32 can accumulate in the nucleus. *Biochem Biophys Res Commun* **281**, 1161–1169.

Buchkovich, N. J., Maguire, T. G. & Alwine, J. C. (2010). Role of the endoplasmic reticulum chaperone BiP, SUN domain proteins, and dynein in altering nuclear morphology during human cytomegalovirus infection. *J Virol* **84**, 7005–7017.

Chou, S., Hakki, M. & Villano, S. (2012). Effects on maribavir susceptibility of cytomegalovirus UL97 kinase ATP binding region mutations detected after drug exposure *in vitro* and *in vivo*. *Antiviral Res* **95**, 88–92.

Dolan, A., Cunningham, C., Hector, R. D., Hassan-Walker, A. F., Lee, L., Addison, C., Dargan, D. J., McGeoch, D. J., Gatherer, D. & other authors (2004). Genetic content of wild-type human cytomegalovirus. *J Gen Virol* **85**, 1301–1312.

Ellsmore, V., Reid, G. G. & Stow, N. D. (2003). Detection of human cytomegalovirus DNA replication in non-permissive Vero and 293 cells. *J Gen Virol* **84**, 639–645.

Feichtinger, S., Stamminger, T., Müller, R., Graf, L., Klebl, B., Eickhoff, J. & Marschall, M. (2011). Recruitment of cyclin-dependent kinase 9 to nuclear compartments during cytomegalovirus late replication: importance of an interaction between viral pUL69 and cyclin T1. *J Gen Virol* **92**, 1519–1531.

Gebert, S., Schmolke, S., Sorg, G., Flöss, S., Plachter, B. & Stamminger, T. (1997). The UL84 protein of human cytomegalovirus acts as a transdominant inhibitor of immediate-early-mediated trans-activation that is able to prevent viral replication. *J Virol* **71**, 7048–7060.

Graf, L., Webel, R., Wagner, S., Hamilton, S. T., Rawlinson, W. D., Sticht, H. & Marschall, M. (2013). The cyclin-dependent kinase ortholog pUL97 of human cytomegalovirus interacts with cyclins. *Viruses* **5**, 3213–3230.

Grimm, K. S., Klupp, B. G., Granzow, H., Müller, F. M., Fuchs, W. & Mettenleiter, T. C. (2012). Analysis of viral and cellular factors influencing herpesvirus-induced nuclear envelope breakdown. *J Virol* **86**, 6512–6521.

Hamilton, S. T., Milbradt, J., Marschall, M. & Rawlinson, W. D. (2014). Human cytomegalovirus replication is strictly inhibited by siRNAs targeting UL54, UL97 or UL122/123 gene transcripts. *PLoS One* **9**, e97231.

Hamirally, S., Kamil, J. P., Ndassa-Colday, Y. M., Lin, A. J., Jahng, W. J., Baek, M. C., Noton, S., Silva, L. A., Simpson-Holley, M. & other authors (2009). Viral mimicry of Cdc2/cyclin-dependent kinase 1 mediates disruption of nuclear lamina during human cytomegalovirus nuclear egress. *PLoS Pathog* **5**, e1000275.

Hertel, L., Chou, S. & Mocarski, E. S. (2007). Viral and cell cycle-regulated kinases in cytomegalovirus-induced pseudomitosis and replication. *PLoS Pathog* **3**, e6.

Hume, A. J., Finkel, J. S., Kamil, J. P., Coen, D. M., Culbertson, M. R. & Kalejta, R. F. (2008). Phosphorylation of retinoblastoma protein by viral protein with cyclin-dependent kinase function. *Science* **320**, 797–799.

Hutterer, C., Eickhoff, J., Milbradt, J., Korn, K., Zeitträger, I., Bahsi, H., Wagner, S., Zischinsky, G., Wolf, A. & other authors (2015). A novel CDK7 inhibitor of the Pyrazolotriazine class exerts broad-spectrum antiviral activity at nanomolar concentrations. *Antimicrob Agents Chemother* **59**, 2062–2071.

Johnson, D. C. & Baines, J. D. (2011). Herpesviruses remodel host membranes for virus egress. *Nat Rev Microbiol* **9**, 382–394.

Klupp, B. G., Granzow, H. & Mettenleiter, T. C. (2011). Nuclear envelope breakdown can substitute for primary envelopment-mediated nuclear egress of herpesviruses. *J Virol* **85**, 8285–8292.

Krosky, P. M., Baek, M. C. & Coen, D. M. (2003). The human cytomegalovirus UL97 protein kinase, an antiviral drug target, is required at the stage of nuclear egress. *J Virol* **77**, 905–914.

Leach, N. R. & Roller, R. J. (2010). Significance of host cell kinases in herpes simplex virus type 1 egress and lamin-associated protein disassembly from the nuclear lamina. *Virology* **406**, 127–137.

Lemnitzer, F., Raschbichler, V., Kolodziejczak, D., Israel, L., Imhof, A., Bailer, S. M., Koszinowski, U. & Ruzsics, Z. (2013). Mouse cytomegalovirus egress protein pM50 interacts with cellular endophilin-A2. *Cell Microbiol* **15**, 335–351.

Lye, M. F., Sharma, M., El Omari, K., Filman, D. J., Schuermann, J. P., Hogle, J. M. & Coen, D. M. (2015). Unexpected features and mechanism of heterodimer formation of a herpesvirus nuclear egress complex. *EMBO J*, e201592651.

Marschall, M., Marzi, A., aus dem Siepen, P., Jochmann, R., Kalmer, M., Auerochs, S., Lischka, P., Leis, M. & Stamminger, T. (2005). Cellular p32 recruits cytomegalovirus kinase pUL97 to redistribute the nuclear lamina. *J Biol Chem* **280**, 33357–33367.

Marschall, M., Feichtinger, S. & Milbradt, J. (2011). Regulatory roles of protein kinases in cytomegalovirus replication. *Adv Virus Res* **80**, 69–101.

Mettenleiter, T. C., Müller, F., Granzow, H. & Klupp, B. G. (2013). The way out: what we know and do not know about herpesvirus nuclear egress. *Cell Microbiol* **15**, 170–178.

Milbradt, J., Auerochs, S. & Marschall, M. (2007). Cytomegaloviral proteins pUL50 and pUL53 are associated with the nuclear lamina and interact with cellular protein kinase C. *J Gen Virol* **88**, 2642–2650.

Milbradt, J., Auerochs, S., Sticht, H. & Marschall, M. (2009). Cytomegaloviral proteins that associate with the nuclear lamina: components of a postulated nuclear egress complex. *J Gen Virol* **90**, 579–590.

Milbradt, J., Webel, R., Auerochs, S., Sticht, H. & Marschall, M. (2010). Novel mode of phosphorylation-triggered reorganization of the nuclear lamina during nuclear egress of human cytomegalovirus. *J Biol Chem* **285**, 13979–13989.

Milbradt, J., Auerochs, S., Sevvana, M., Muller, Y. A., Sticht, H. & Marschall, M. (2012). Specific residues of a conserved domain in the N terminus of the human cytomegalovirus pUL50 protein determine its intranuclear interaction with pUL53. *J Biol Chem* **287**, 24004–24016.

Milbradt, J., Kraut, A., Hutterer, C., Sonntag, E., Schmeiser, C., Ferro, M., Wagner, S., Lenac, T., Claus, C. & other authors (2014). Proteomic analysis of the multimeric nuclear egress complex of human cytomegalovirus. *Mol Cell Proteomics* **13**, 2132–2146.

Mocarski, E. S., Shenk, T., Griffiths, P. D. & Pass, R. F. (2013). Cytomegaloviruses. In *Fields Virology*, pp. 1960–2014. Edited by D. M. Knipe & P. M. Howley. Philadelphia, PA: Lippincott Williams and Wilkins.

Muranyi, W., Haas, J., Wagner, M., Krohne, G. & Koszinowski, U. H. (2002). Cytomegalovirus recruitment of cellular kinases to dissolve the nuclear lamina. *Science* **297**, 854–857.

Ogawa-Goto, K., Tanaka, K., Gibson, W., Moriishi, E., Miura, Y., Kurata, T., Irie, S. & Sata, T. (2003). Microtubule network facilitates nuclear targeting of human cytomegalovirus capsid. *J Virol* **77**, 8541–8547.

Prichard, M. N., Gao, N., Jairath, S., Mulamba, G., Krosky, P., Coen, D. M., Parker, B. O. & Pari, G. S. (1999). A recombinant human cytomegalovirus with a large deletion in UL97 has a severe replication deficiency. *J Virol* **73**, 5663–5670.

Rechter, S., Scott, G. M., Eickhoff, J., Zielke, K., Auerochs, S., Müller, R., Stamminger, T., Rawlinson, W. D. & Marschall, M. (2009). Cyclin-dependent kinases phosphorylate the cytomegalovirus RNA export protein pul69 and modulate its nuclear localization and activity. *J Biol Chem* **284**, 8605–8613.

Sam, M. D., Evans, B. T., Coen, D. M. & Hogle, J. M. (2009). Biochemical, biophysical, and mutational analyses of subunit interactions of the human cytomegalovirus nuclear egress complex. *J Virol* **83**, 2996–3006.

Sanchez, V. & Spector, D. H. (2006). Cyclin-dependent kinase activity is required for efficient expression and posttranslational modification of human cytomegalovirus proteins and for production of extracellular particles. *J Virol* **80**, 5886–5896.

Sandal, T., Stapnes, C., Kleivdal, H., Hedin, L. & Døskeland, S. O. (2002). A novel, extraneuronal role for cyclin-dependent protein kinase 5 (CDK5): modulation of cAMP-induced apoptosis in rat leukemia cells. *J Biol Chem* **277**, 20783–20793.

Schang, L. M., Coccaro, E. & Lacasse, J. J. (2005). Cdk inhibitory nucleoside analogs prevent transcription from viral genomes. *Nucleosides Nucleotides Nucleic Acids* **24**, 829–837.

Schmeiser, C., Borst, E., Sticht, H., Marschall, M. & Milbradt, J. (2013). The cytomegalovirus egress proteins pUL50 and pUL53 are translocated to the nuclear envelope through two distinct modes of nuclear import. *J Gen Virol* **94**, 2056–2069.

Schregel, V., Auerochs, S., Jochmann, R., Maurer, K., Stamminger, T. & Marschall, M. (2007). Mapping of a self-interaction domain of the cytomegalovirus protein kinase pUL97. *J Gen Virol* **88**, 395–404.

Sharma, M., Bender, B. J., Kamil, J. P., Lye, M. F., Pesola, J. M., Reim, N. I., Hogle, J. M. & Coen, D. M. (2015). Human cytomegalovirus UL97 phosphorylates the viral nuclear egress complex. *J Virol* **89**, 523–534.

Soni, D. V. & Jacobberger, J. W. (2004). Inhibition of cdk1 by alsterpaullone and thioflavopiridol correlates with increased transit time from mid G2 through prophase. *Cell Cycle* **3**, 349–357.

Steingruber, M., Socher, E., Hutterer, C., Webel, R., Bergbrede, T., Lenac, T., Sticht, H. & Marschall, M. (2015). The interaction between cyclin B1 and cytomegalovirus protein kinase pUL97 is determined by an active kinase domain. *Viruses* **7**, 4582–4601.

Trofe, J., Pote, L., Wade, E., Blumberg, E. & Bloom, R. D. (2008). Maribavir: a novel antiviral agent with activity against cytomegalovirus. *Ann Pharmacother* **42**, 1447–1457.

Walzer, S. A., Egerer-Sieber, C., Sticht, H., Sevvana, M., Hohl, K., Milbradt, J., Muller, Y. A. & Marschall, M. (2015). Crystal structure of the human cytomegalovirus pul50-pul53 core nuclear egress complex provides insight into a unique assembly scaffold for virus-host protein interactions. *J Biol Chem* **290**, 27452–27458.

Wolf, D. G., Courcelle, C. T., Prichard, M. N. & Mocarski, E. S. (2001). Distinct and separate roles for herpesvirus-conserved UL97 kinase in cytomegalovirus DNA synthesis and encapsidation. *Proc Natl Acad Sci U S A* **98**, 1895–1900.